

# Effect of Premade Compatibilizer and Reactive Polymers on Polystyrene Drop Deformation and Breakup in Simple Shear

Bin Lin,<sup>†</sup> Frej Mighri,<sup>‡</sup> Michel A. Huneault,<sup>§</sup> and Uttandaraman Sundararaj<sup>\*,†</sup>

Department of Chemical and Materials Engineering, University of Alberta, Edmonton, Canada T6G 2G6; Department of Chemical Engineering, Laval University, Sainte-Foy, Quebec, Canada G1K 7P4; and Industrial Materials Institute, National Research Council Canada, 75 Boulevard de Mortagne, Boucherville, Canada J4B 6Y4

Received November 17, 2004; Revised Manuscript Received April 22, 2005

**ABSTRACT:** The deformation and breakup of a single polymer drop with compatibilizer (premade or in-situ) inside a polymer matrix was visualized at high temperature under simple shear in a specially designed transparent Couette mixer. The compatibilized systems were polyethylene/polystyrene (PE/PS) with polyethylene-*block*-polystyrene copolymer (P(E-*b*-S)) and polystyrene oxazoline (PSOX) with polyethylene maleic anhydride (PEMA). The uncompatibilized polymer systems studied were PE/PS and PE/PSOX. With or without compatibilizer, the drop elongated in the vorticity direction and then broke up in that direction. In the presence of premade or reactively formed compatibilizer, drop breakup occurs at a shear rate similar to that in the uncompatibilized systems, which suggests that copolymer does not affect initial polymer drop breakup greatly. Interfacial cross-linking in reactive systems stabilized the drop by forming a tiny cylindrical tip in the vorticity direction. Consequently, drop erosion and vorticity elongation and breakup occurred at a much higher shear rate compared to the nonreactive systems.

## Introduction

Polymer blends provide an effective and economical way to create new materials.<sup>1,2</sup> Most polymer pairs are immiscible and therefore need to be compatibilized.<sup>3</sup> Compatibilization is a process that modifies the interfacial properties of immiscible blends and stabilizes the desired morphology; therefore, it can affect the final properties of the blends.

Studies on how compatibilizer affects drop deformation and breakup are few. Levitt and Macosko<sup>4</sup> sheared polypropylene (PP) drops and poly(methyl methacrylate) (PMMA) drops inside polystyrene (PS) matrix with a counter-rotating parallel plate device and found that drop cross-sectional area increased when a block copolymer (10 wt % based on the drop phase) was added. They attributed this increase to either a reduction in interfacial tension or a reduction in slip. It might also be due to a combination of these two effects and a gradient in interfacial tension. van Puyvelde et al.<sup>5</sup> studied model blends composed of 1% polyisobutene (PIB) in poly(dimethylsiloxane) (PDMS) with PIB–PDMS diblock copolymer in a shearing cell. They saw the PIB drop with 2% copolymer showed pointed ends in the velocity direction during shearing and ascribed this to the accumulation of block copolymer at the drop tips. They suggested this accumulation resulted in a lower local interfacial stress, giving a higher local curvature to balance the pressure jump across the interface. This is consistent with rheological results.<sup>6</sup> van Puyvelde et al.<sup>5</sup> also found that the PIB drop with 10% copolymer had almost no deformation. They explained that this was due to the strong Marangoni stress, which immobilized the interface at high surface

coverage. More recently, Jeon and Macosko<sup>7</sup> visualized block copolymer distribution on a sheared polymer drop by using a fluorescent labeled poly(styrene-*b*-methyl methacrylate) (NBD-PS-*b*-PMMA). They observed higher block copolymer concentration at the drop edges and tips—this was thought to be due to the convection of block copolymer induced by shear flow.

It has been thought that the role of the compatibilizers (or surfactants in emulsions) (for example, refs 8–10) is to lower the interfacial tension and therefore to facilitate drop breakup. For Newtonian systems, in the presence of compatibilizers or surfactants, drop deformation increased at a given capillary number (where capillary number is the ratio of the viscous stress to the interfacial stress). With compatibilizer, the critical capillary number for drop deformation and breakup decreased, and tip streaming was observed. Tip streaming is a phenomenon where streams of small droplets are released in the flow direction from the tips of a pointed drop. However, other studies<sup>11–13</sup> showed that the compatibilized drops were more stable against breakup and coalescence. Therefore, the effects of compatibilizers on drop breakup are still not well understood.

An important parameter often used in characterizing drop breakup is the viscosity ratio. Viscosity ratio,  $\eta_r$ , is a ratio of the drop phase viscosity to the matrix phase viscosity. We have shown in our previous work<sup>14–16</sup> that polymer drops can break up at a viscosity ratio higher than 4, which is impossible in Newtonian systems.<sup>17,18</sup> Figure 1 shows four kinds of breakup mechanisms seen in polymer systems, namely: (1) “erosion”—surface erosion<sup>15,19</sup> from the drop in the form of thin ribbons and streams of small droplets;<sup>15</sup> (2) “parallel breakup”—the drop breaks after being stretched into a thin sheet<sup>16,20–26</sup> or a flat sausage<sup>14</sup> parallel to the flow direction;<sup>14,16</sup> (3) “vorticity elongation and breakup”—the drop breaks after being elongated in the vorticity direction;<sup>14,27–32</sup> (4) “tip streaming”—a well-

<sup>†</sup> University of Alberta.

<sup>‡</sup> Laval University.

<sup>§</sup> National Research Council Canada.

\* To whom correspondence should be addressed: e-mail u.sundararaj@ualberta.ca; phone 1-780-492-1044; fax 1-780-492-2881.

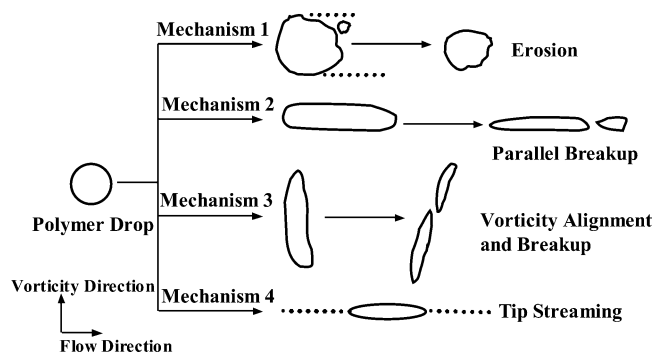


**Figure 1.** Polymer drop breakup mechanisms subjected to simple shear flow.

known breakup mechanism even in Newtonian systems.<sup>8–10,17,18,33–37</sup> Besides “tip streaming”, all other mechanisms are unique to viscoelastic systems. In this paper, we observe the effects of compatibilization on polymer drop deformation and breakup using a transparent Couette mixer.

## Experimental Section

**Materials.** The polymer systems consisted of polystyrene (PS) drops or polystyrene oxazoline (PSOX) chunks inside a polyethylene (PE) matrix. Two grades of PE were used, PE1 and PE2. The diblock copolymer polystyrene-*block*-polyethylene (P(S-*b*-E)) was used as compatibilizer for the PE/PS system. For the PE/PSOX system, polyethylene maleic anhydride (PEMA) was added into PE matrix to generate a reactive system. The P(S-*b*-E) copolymer came in powder form and was synthesized by researchers at University of Minnesota. It is a symmetric block copolymer with a molecular weight ( $M_n$ ) of 100–100 kg/mol.<sup>38</sup>

All the other polymers were obtained in pellet form from commercial sources. Table 1 lists physical properties and sources of the homopolymers used. The molecular weight data of PEMA were provided by DuPont Canada, and the molecular weight data of other polymers used were measured with size-exclusion chromatography (SEC) using an Alliance 2000 GPCV equipped with a series of three Waters HT6E columns (Waters Chromatography Division, Millipore, Milford, MA). Dynamic rheological characterizations were performed using a Rheometrics RMS800 rheometer with a 25 mm parallel plate fixture operated at 10% strain. Figure 2 shows the complex viscosity and elastic modulus for polymers used in this study. The interfacial tension between PS and PE at 190 °C is 4.9 mN/m.<sup>40</sup> This interfacial tension is used to calculate capillary number for all systems.

The PS spherical drops were specially prepared in silicone oil. The detailed procedure can be found in ref 15. To avoid reaction of the oxazoline group during the heating process of drop preparation, the PSOX was added to the Couette device as nonspherical chunks directly after cutting the pellets. Drops with diblock copolymer, P(S-*b*-E), were prepared in two ways. One method was to premix 1 or 5 wt % P(S-*b*-E) with PS in an APAM mini-mixer<sup>41</sup> at 190 °C and 50 rpm. The other was to insert a PS drop dry coated with P(S-*b*-E) into a PE pellet. The maximum interfacial coverage,  $\Sigma_{\max}$ , for 100–100 kg/mol P(S-*b*-E) is estimated to be 0.15 chain/nm<sup>2</sup>, based on  $\Sigma_{\max} = 0.25$  chain/nm<sup>2</sup> for 20–20 kg/mol P(S-*b*-E)<sup>38</sup> and the scaling rule<sup>42</sup>  $\Sigma_{\max} \sim M_n^{-1/3}$ . This maximum interfacial coverage corresponds to only 0.06 wt % of copolymer for a 0.5 mm diameter PS drop if all the copolymer distributes at the drop surface without micelle formation.

It should be noted that the viscous and elastic moduli of PS + 5% P(S-*b*-E) are lower than those of PS (see Figure 2), but the viscous and elastic modulus of PS + 1% P(S-*b*-E) are greater than those of PS. According to Jones et al.,<sup>43</sup> a possible reason for change in the moduli and/or viscosity is due to the extent of homopolymer penetration into the copolymer mi-

celles. If the micelles act as inert spheres where the micellar corona behaves as a dry brush, the viscosity increases. On the other hand, if the micelles work as plasticizers where the corona becomes “wet”, the viscosity decreases. In this paper, we use the measured rheology data for PS premixed with P(S-*b*-E) and estimate the rheology of PS coated with P(S-*b*-E) using pure PS data.

**Setup.** The specially designed transparent Couette flow cell consists of two counter-rotating concentric cylinders. A detailed description of the setup can be found elsewhere.<sup>30</sup> The transparent outer cylinder is made of quartz and is heated with infrared heaters, while the inner cylinder is made of stainless steel and is heated uniformly by six cartridge heaters. The drop deformation and breakup processes are recorded using a high-resolution digital camcorder Canon XL1. In the present Couette setup, the visualization plane is the plane containing the flow direction and the vorticity axis.

**Experimental Procedure.** At the beginning of each run, the Couette cell was preheated to 125 °C. The gap of the Couette cell was then filled with PE pellets premixed with a small amount of thermal stabilizer (Irganox 1076), from Ciba Chemicals, and 4–6 PS spheres or PSOX chunks were inserted carefully into PE matrix. When PEMA was used, the PSOX drop phase was inserted into a PEMA pellet first before it was added to the Couette apparatus.

Experiments were performed by increasing shear rate stepwise at a constant temperature of 190 °C. The drop deformation and breakup were recorded and then subsequently analyzed using Adobe Photoshop software. Drop images at particular deformation times were grabbed, and their dimensions were measured based on prior calibration.

## Results

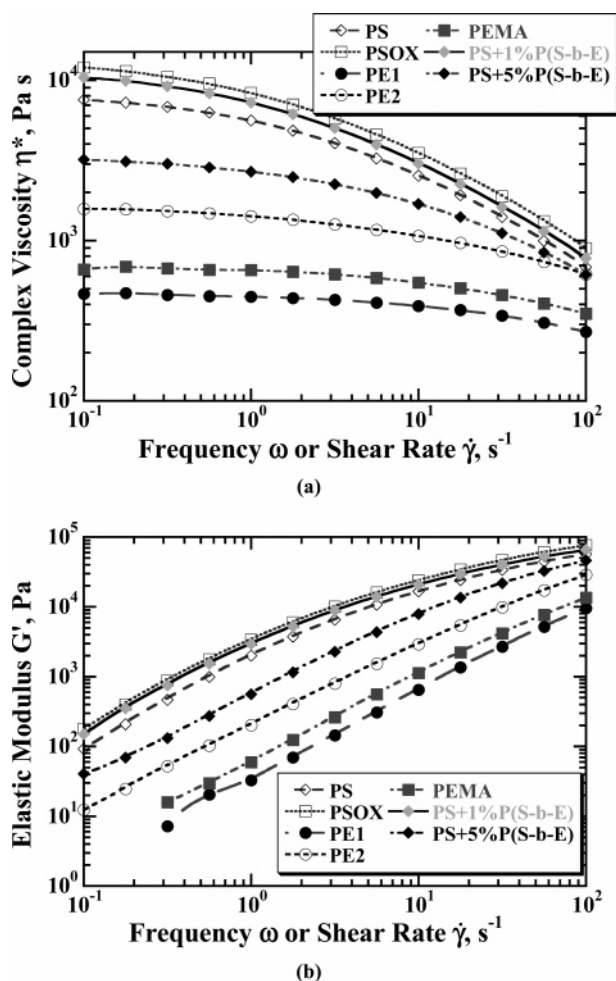
**Premade Compatibilizer.** Figure 3 shows a series of micrographs of an uncompatibilized PS drop ( $D_0 = 0.52$  mm) deforming and breaking up in the PE1 matrix. Initially, the PS drop is quite spherical (Figure 3a). Tip streaming occurs when the shear rate is increased to 3 s<sup>-1</sup>, and small drops come off the mother drop in the flow direction. At this point, the viscosity ratio is 10. When the shear rate is further increased to 4 s<sup>-1</sup>, the drop is first stretched into a sausage shape (Figure 3b) and then breaks up into two daughter droplets (Figure 3c); that is, it breaks up via mechanism 2 (see Figure 1 and ref 16). We then follow the daughter droplet on the left side of the image in Figure 3c ( $D \approx 0.35$  mm). The droplet continuously elongates in the vorticity direction. The vorticity alignment and elongation, like the rod-climbing Weissenberg phenomenon, is attributed to high normal stress in polymers.<sup>27–30</sup> No breakup occurs even when the shear rate is increased to 8 s<sup>-1</sup> (Figure 3d).

Figure 4 shows micrographs of the deformation and breakup of a PS drop premixed with 5% P(S-*b*-E). The system has a lower viscosity ratio than that of PE1/PS (see Figure 2). The drop, with a diameter of 0.58 mm, has already begun to deform at the beginning of the recording (Figure 4a). Tip streaming (mechanism 4 in Figure 1 and ref 14) is observed at  $\dot{\gamma} \approx 3$  s<sup>-1</sup>, and then, the drop begins to elongate in the vorticity direction. When the shear rate is increased to 4 s<sup>-1</sup>, less tip streaming is observed (Figure 4b), but the drop still elongates in the vorticity direction. After about 360 s at this shear rate, the drop breaks up into two daughter droplets via vorticity elongation at a shear rate of 4 s<sup>-1</sup> (Figure 4c, breakup mechanism 3 in Figure 1 and ref 14). This vorticity breakup occurs at a similar shear rate as the uncompatibilized drop, though the breakup type is different. We then followed the lower daughter droplet ( $D \approx 0.35$  mm) in Figure 4c that had a tiny elastic cylindrical tip at the top of the droplet. The tip breaks

Table 1. Properties of Homopolymers Used

polymer: commercial name (abbreviation)	source	molecular weight		viscosity at $\dot{\gamma} = 1 \text{ s}^{-1}$ , $T = 190 \text{ }^{\circ}\text{C}$ (Pa·s)	density $\rho$ (kg/m <sup>3</sup> ) <sup>a</sup>	refractive index <sup>b</sup>
		$M_n$ (g/mol)	$M_w$ (g/mol)			
polystyrene: STYRON 666 (PS)	Dow	97 000	160 000	4500	1040 (25 °C)	1.59
polystyrene oxazoline (PSOX, 1% oxazoline)	Dow		160 000	8300		1.66
polyethylene: DMDA-8920 (PE1)	Petromont	14 400	53 400	450	954 (25 °C)	1.49
polyethylene: DMDB-8907 (PE2)	Petromont	19 800	68 900	1400	952 (25 °C)	1.49
polyethylene maleic anhydride: Fusabond MB265D (PEMA, 1% MAH)	DuPont	21 100 <sup>a</sup>	48 400 <sup>a</sup>	650	950 (25 °C)	1.55

<sup>a</sup> Provided by supplier. <sup>b</sup> Reference 39.



**Figure 2.** (a) Complex viscosity and (b) elastic modulus at 190 °C of polymers used in this study.

off from the droplet at a shear rate of  $7 \text{ s}^{-1}$  (Figure 4d). An elastic tip extending from the drop is also observed for PS premixed with 1% P(S-b-E) drop (not shown).

The tiny elastic cylindrical tip found during drop deformation and breakup (Figure 4c,d) is somewhat similar to what was observed by van Puyvelde et al.<sup>5</sup> However, the tip in the work by van Puyvelde et al.<sup>5</sup> was in the flow direction while the tip in our work was in the vorticity direction. van Puyvelde et al.<sup>5</sup> showed that a drop composed of PIB premixed with 2% PIB-PDMS copolymer exhibited pointed ends in the flow direction when the drop was sheared inside PDMS. In their experiments, the viscosity ratio was close to 1, both drop and matrix phases were nearly Newtonian without noticeable elasticity, and the drop had a diameter on the order of a micron. Therefore, shear stress and

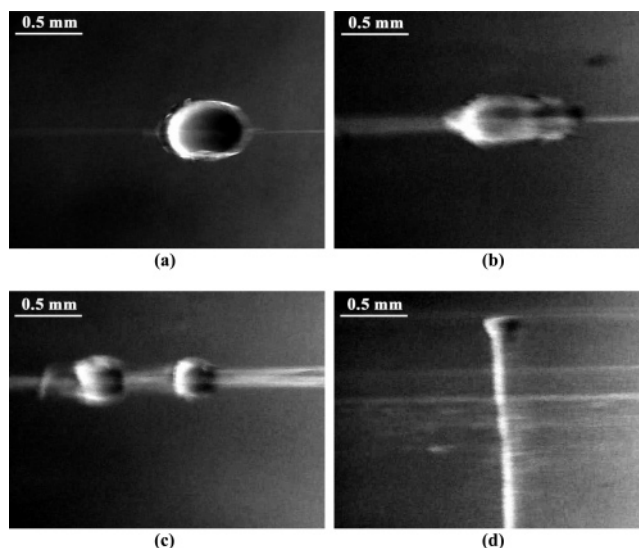


**Figure 3.** Deformation and breakup of a PS drop ( $D_0 = 0.52 \text{ mm}$ ) in a PE1 matrix at 190 °C subject to a stepwise shear rate increase. Time and conditions for each figure: (a)  $t = 5 \text{ s}$ ,  $\dot{\gamma} = 0.3 \text{ s}^{-1}$ ,  $\eta_r = 15$ ; (b)  $t = 535 \text{ s}$ ,  $\dot{\gamma} = 4.4 \text{ s}^{-1}$ ,  $\eta_r = 9$ ; (c)  $t = 541 \text{ s}$ ,  $\dot{\gamma} = 4.0 \text{ s}^{-1}$ ,  $\eta_r = 9$ ; (d)  $t = 1547 \text{ s}$ ,  $\dot{\gamma} = 8.4 \text{ s}^{-1}$ ,  $\eta_r = 7$ . Note scale bar. For the micrographs, the flow direction is horizontal and the vorticity direction is vertical.

interfacial stress are the two important factors in their case. In our experiments, we saw that the tiny tip developed in the vorticity direction. The possible reasons are that both PS drops and PE matrix have high viscous and elastic moduli (see Figure 2). The drop phase has much higher moduli than those of the matrix phase, with both viscosity ratio and elastic ratio ( $G'_d/G'_m$ ) higher than 5, and the drop diameter is on the order of a millimeter. For a 0.5 mm PS drop subjected to a shear rate of  $10 \text{ s}^{-1}$  in a PE1 matrix, interfacial stress ( $\Gamma/R$ ) is on the order of  $10 \text{ N/m}^2$  and shear stress ( $\eta_m \dot{\gamma}$ ) is on the order of  $1000 \text{ N/m}^2$ . Therefore, in these experiments, shear stress and normal stresses may dominate. As a result, phenomena such as drop alignment and elongation in vorticity axis<sup>14,27–32</sup> due to normal stresses are observed. A detailed explanation on the tiny tip will be shown in the Discussion section.

Figure 5 shows the deformation and breakup of a PS drop with a diameter of 0.53 mm dry-coated with P(S-b-E). For compatibilized drop preparation in this way, we do not know the exact mass of the copolymer added. According to the group contribution method,<sup>39</sup> the densities of PS and PE at 190 °C are 990 and 860 kg/m<sup>3</sup>, respectively. The weight of the copolymer at the drop surface is estimated by using the arithmetic average density of PS and PE. The drop surface copoly-



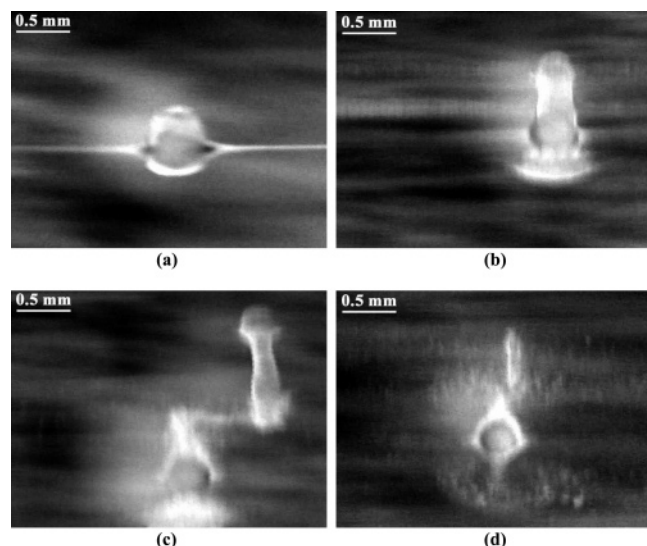


**Figure 4.** Premade copolymer. Deformation and breakup of a PS + 5% P(S-*b*-E) drop ( $D_0 = 0.58$  mm) in a PE1 matrix at 190 °C subject to a stepwise shear rate increase. Time and conditions for each figure: (a)  $t = 0$  s,  $\dot{\gamma} = 3.0$  s $^{-1}$ ,  $\eta_r = 5$ ; (b)  $t = 126$  s,  $\dot{\gamma} = 3.6$  s $^{-1}$ ,  $\eta_r = 5$ ; (c)  $t = 480$  s,  $\dot{\gamma} = 3.8$  s $^{-1}$ ,  $\eta_r = 5$ ; (d)  $t = 669$  s,  $\dot{\gamma} = 6.6$  s $^{-1}$ ,  $\eta_r = 5$ . Note scale bar. For the micrographs, the flow direction is horizontal and the vorticity direction is vertical.

mer concentration is found using

$$\frac{\text{mass of copolymer}}{\text{mass of drop} + \text{mass of copolymer}} = \frac{[\text{density} \times \text{volume}]_{\text{bcp}}}{[\text{density} \times \text{volume}]_{\text{PS}} + [\text{density} \times \text{volume}]_{\text{bcp}}} \quad (1)$$

Since all the copolymer is added at the drop surface and the average thickness of the copolymer powder added at the drop surface is probably close to 0.01 mm, the drop surface copolymer concentration will be around 5 wt % based on the drop, much greater than the maximum coverage concentration (0.06 wt %). Though it is difficult to tell whether the interface between the drop and the matrix phase is saturated with copolymer or not, enough copolymer was added to saturate the drop surface if all the copolymer powder stays at the interface and no micelles are formed.

Tip streaming is observed at a shear rate of 2 s $^{-1}$  (Figure 5a). After  $t \approx 800$  s, the drop interface becomes obscure (Figure 5b), and the 2D cross-sectional area is around 1.2 times that of the initial drop. This may be because the drop has flattened in the direction perpendicular to the viewing plane. Figure 5c shows that the drop elongates in the vorticity direction continuously. It breaks up into two daughter droplets at  $\dot{\gamma} \approx 3$  s $^{-1}$  (see Figure 5d). Though the addition of compatibilizer allows the drop to break up at a slightly lower shear rate than the uncompatibilized case, the shear rates are comparable. We followed the deformation and breakup of the daughter droplet at the top of the image in Figure 5d ( $D \approx 0.42$  mm). When the shear rate is increased to 6 s $^{-1}$ , it, like the mother drop, aligns and elongates in the vorticity direction (Figure 5e). More elongation is observed when the shear rate is increased to 7 s $^{-1}$ . Figure 5f shows the breakup of the daughter droplet (see bottom of Figure 5f).

The increase in drop cross-sectional area with copolymer present at the interface has also been observed by

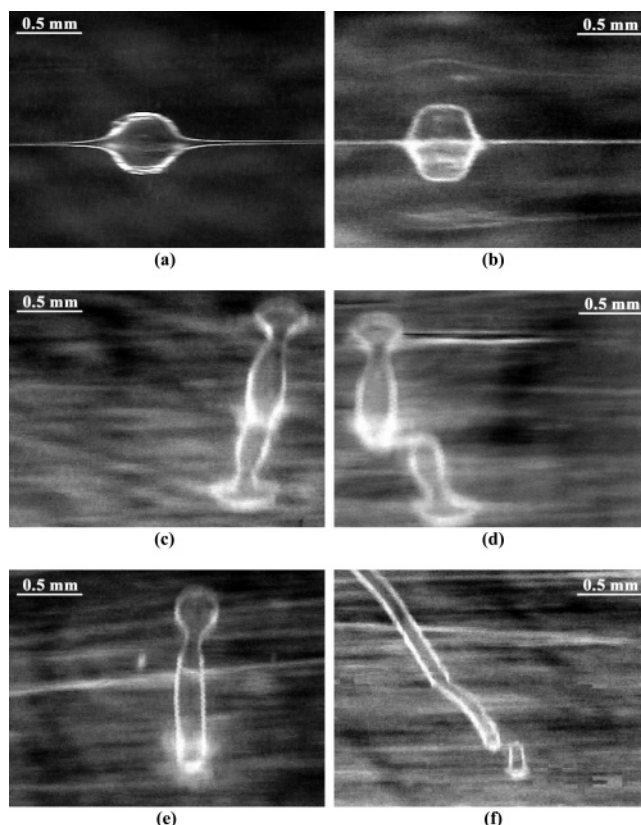


**Figure 5.** Premade copolymer. Deformation and breakup of a PS drop ( $D_0 = 0.53$  mm) coated with P(S-*b*-E) in a PE1 matrix at 190 °C subject to a stepwise shear rate increase. Time and conditions for each figure: (a)  $t = 114$  s,  $\dot{\gamma} = 2.3$  s $^{-1}$ ,  $\eta_r \approx 10$ ; (b)  $t = 801$  s,  $\dot{\gamma} = 2.3$  s $^{-1}$ ,  $\eta_r \approx 10$ ; (c)  $t = 1124$  s,  $\dot{\gamma} = 2.3$  s $^{-1}$ ,  $\eta_r \approx 10$ ; (d)  $t = 1158$  s,  $\dot{\gamma} = 3.4$  s $^{-1}$ ,  $\eta_r \approx 9$ ; (e)  $t = 1291$  s,  $\dot{\gamma} = 6.0$  s $^{-1}$ ,  $\eta_r \approx 8$ ; (f)  $t = 1665$  s,  $\dot{\gamma} = 7.4$  s $^{-1}$ ,  $\eta_r \approx 7$ . Note scale bar. For the micrographs, the flow direction is horizontal and the vorticity direction is vertical.

Levitt and Macosko.<sup>4</sup> In their experiments,<sup>4</sup> the drop was generated by breaking up a polymer fiber with 10% block copolymer (used as the drop phase) that was sandwiched between two disks of the other polymer (used as the matrix phase). The sandwiched sample was put into the parallel plate device at the experimental temperature for 1 h before the motors started to rotate. The drop obtained by this method had most of the copolymers distributed evenly at the drop surface before shearing.<sup>7</sup> In our case, when we added copolymer evenly at the drop surface at the beginning of the experiment, the PS drop interface has an almost uniform P(S-*b*-E) layer and the interfacial concentration is much greater ( $\sim 80$  times) than the concentration required for saturation of the drop surface before shearing. There is less concentration gradient for this case vs the drop with premixed copolymer, and the interface may be sufficiently saturated for the coated case so that the interfacial stress around the drop is homogeneous. The copolymer at the interface of the PS drop and PE matrix may also suppress interfacial slip.<sup>44</sup> As a consequence, a drop will be stretched more and thus have a larger cross-sectional area in the viewing plane. A summary on the drop deformation and breakup data is shown in Table 2.

**Interfacial Cross-Linking Reaction.** Figure 6 shows the deformation and breakup of a PSOX chunk ( $D \approx 0.66$  mm) inside a PE2 matrix. Parts a, c, e, g of Figure 6 are the images at different mixing times, and parts

Table 2. Summary on Drop Deformation and Breakup

matrix/drop	$D$ (mm)	$\dot{\gamma}$ ( $\text{s}^{-1}$ )	$\eta_r$	Ca	De	breakup mode	notes
PE1/PS	0.52	3.0	10	68	3.0	tip streaming	
	0.52	4.0	9	90	4.0	parallel breakup	
	0.36	8.4	7	123	8.4	vorticity alignment	
PE1/PS + 1% P(S- <i>b</i> -E)	0.51	4.4	11	96	5.5	tiny cylindrical tip breaks off	no breakup at this shear rate cylindrical tip along the vorticity axis develops at $4.4 \text{ s}^{-1}$
	0.51	6.5	9	138	8.1	vorticity breakup	
PE1/PS + 5% P(S- <i>b</i> -E)	0.58	3.0	5	76	1.5	tip streaming	
	0.58	3.8	5	95	1.9	vorticity breakup	
	0.35	6.6	5	96	3.3	tiny cylindrical tip breaks off	cylindrical tip along the vorticity axis develops at $3.8 \text{ s}^{-1}$
PE1/PS + P(S- <i>b</i> -E) (dry-coated)	0.53	2.3	$\sim 10$	$\sim 54$	$\sim 2.3$	tip streaming	the viscosity of the drop phase is estimated from PS
	0.53	3.4	$\sim 9$	$\sim 80$	$\sim 3.4$	vorticity breakup	
	0.42	7.4	$\sim 7$	$\sim 128$	$\sim 7.4$	vorticity breakup	
PE1/PSOX	0.52	1.1	18	26	1.5	erosion	the images appear hazy
	0.52	4.7	12	102	6.4	vorticity breakup	
PE1/PSOX + PEMA	0.63	5.6	$\sim 11$	$\sim 148$	$\sim 7.7$	tiny cylindrical tip breaks off	cylindrical tip along the vorticity axis develops at $1.4 \text{ s}^{-1}$
	0.63	7.5	$\sim 10$	$\sim 188$	$\sim 10.3$	erosion	
	0.63	10.5	$\sim 9$	$\sim 263$	$\sim 14.4$	vorticity breakup	the viscosity of the drop phase is estimated from PSOX
PE2/PSOX	0.66	2.3	5	204	3.2	erosion	
	0.66	3.8	4	322	5.2	vorticity breakup	
	0.39	5.5	4	261	7.5	vorticity breakup	
PE2/PSOX + PEMA	0.60	4.1	$\sim 4$	$\sim 308$	$\sim 5.6$	tiny cylindrical tip breaks off	cylindrical tip along the vorticity axis develops at $1.9 \text{ s}^{-1}$
	0.60	6.4	$\sim 4$	$\sim 481$	$\sim 8.8$	erosion	
	0.60	9.7	$\sim 3$	$\sim 641$	$\sim 13.3$	vorticity breakup	the viscosity of the drop phase is estimated from PSOX

b, d, f, h of Figure 6 are the corresponding schematics, which clearly show the drop interface and drop deformation. This is a nonreactive system since PE has no reactive functionality. This run was performed to check the effect of the oxazoline group on breakup without any in-situ reaction. The PSOX chunk aligns in the vorticity direction (Figure 6a), and surface erosion occurs for this elongated drop, with streams of droplets peeling off the mother drop. This PSOX drop subsequently breaks into three droplets at a shear rate of  $4 \text{ s}^{-1}$  (Figure 6c). The center daughter droplet elongates in the vorticity direction (Figure 6e) and breaks up into five droplets (Figure 6g) at a higher shear rate of  $6 \text{ s}^{-1}$ . The PSOX drop may break up at a lower shear rate than the PS drop (see Figure 3) because the PSOX drop is larger and the viscosity ratio is lower for this system than for the PE1/PS system. Similar results were obtained when a PSOX chunk was sheared inside PE1 matrix (see Table 2).

When the PSOX chunk is inserted inside a PEMA pellet and then put into the PE2 matrix, a very different breakup behavior is observed (see Figure 7). The drop viscosity is estimated by PSOX viscosity data and the matrix viscosity using PE2 viscosity data. The PSOX chunk (Figure 7a,  $D \approx 0.60 \text{ mm}$ ) initially aligns and elongates in the vorticity direction (Figure 7b). Almost no erosion is observed at shear rate less than  $4 \text{ s}^{-1}$  (Figure 7a–c). A tiny tip forms at the bottom of the drop, grows, and then breaks up at  $\dot{\gamma} \approx 4 \text{ s}^{-1}$  (Figure 7c). Surface erosion fully develops when the shear rate is increased to  $6 \text{ s}^{-1}$ . The drop breaks up at  $\dot{\gamma} \approx 10 \text{ s}^{-1}$  (Figure 7d); this shear rate is higher than that for the case without reaction (see Figure 6 and Table 2). The same behavior was found when a PSOX chunk inserted inside a PEMA pellet was sheared in a PE1 matrix (see Table 2).

## Discussion

Tip streaming is observed in Newtonian systems with<sup>8–10,12,35</sup> or without<sup>17,18,33–35</sup> surfactants in simple

shear flow. It occurs at viscosity ratios less than 0.1, and breakup occurs at a lower critical capillary number than that for drop fracture.<sup>17,18,33–35</sup> We observed tip streaming in the PE/PS system with or without copolymer even when the viscosity ratio is greater than 3.5, a region where breakup is impossible for Newtonian systems in a simple shear flow field. It has been shown<sup>36,37</sup> that the drop elasticity affects tip streaming in extensional flow fields and occurs even when  $\eta_r > 0.5$  if the drop Deborah number,  $De$ , is greater than 1. The Deborah number is defined as

$$De = \lambda \dot{\gamma} \quad (2)$$

where  $\dot{\gamma}$  is the applied shear rate and  $\lambda$  is the relaxation time of the drop phase. For polymers studied,  $\lambda$  is obtained from the complex viscosity vs frequency data. The intersection of the line representing the zero shear viscosity limit at low frequency and the line representing the power law viscosity at high frequency was determined to be the critical frequency,  $\omega_c$ , and  $\lambda = 1/\omega_c$ . In the PE1/PS system, tip streaming is observed for  $De = 3$  and  $\eta_r = 10$ . This suggests that drop elasticity facilitates polymer drop tip streaming even in a simple shear flow field and that tip streaming can occur at  $\eta_r > 3.5$ , something that is impossible for Newtonian drops.

All tip streaming occurs at a low shear rate  $2\text{--}3 \text{ s}^{-1}$ , which is consistent with other systems we studied.<sup>14</sup> Tip streaming is more prevalent when copolymer is present (see Figures 4 and 5 vs Figure 3). To compare the importance of the convection and the diffusion of the copolymer along the drop interface, the surface Peclet number is usually used:

$$Pe_s = \dot{\gamma} R^2 / D_s \quad (3)$$

where  $R$  is the drop radius and  $D_s$  is the surface diffusivity of the surfactant molecule. At large  $Pe_s$  ( $\gg 1$ ) convection prevails, and at low  $Pe_s$  ( $\ll 1$ ) diffusion

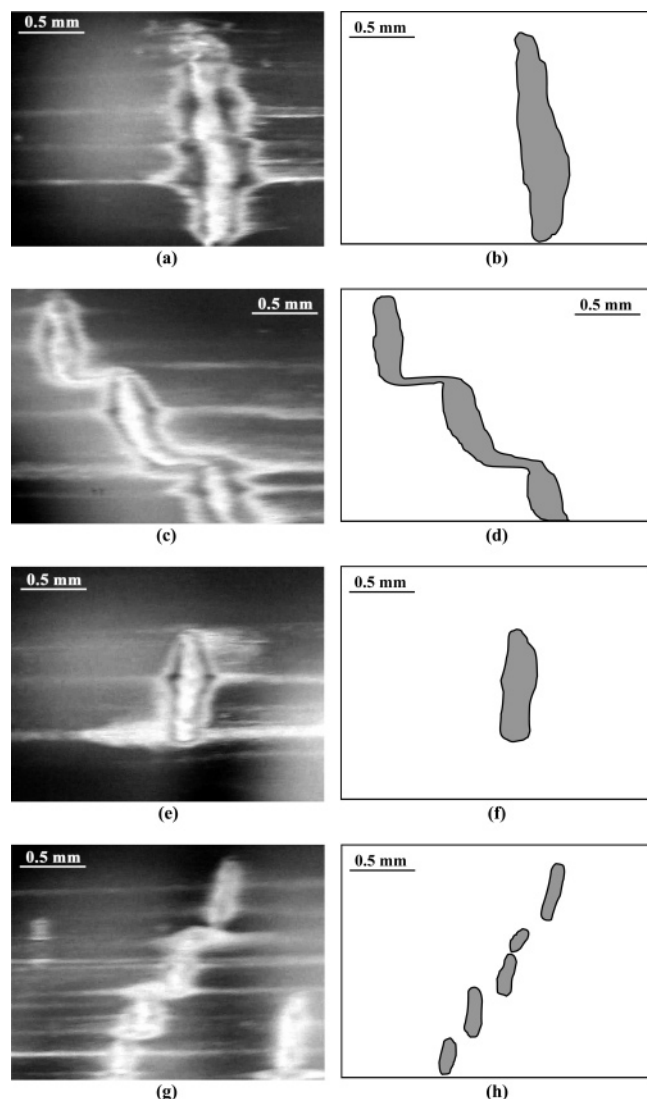


**Figure 6.** Deformation and breakup of a PSOX chunk ( $D_0 \approx 0.67$  mm) in a PE2 matrix at 190 °C subject to a stepwise shear rate increase. Time and conditions for each figure: (a)  $t = 0$  s,  $\dot{\gamma} = 2.3$  s $^{-1}$ ,  $\eta_r \approx 5$ ; (c)  $t = 358$  s,  $\dot{\gamma} = 3.8$  s $^{-1}$ ,  $\eta_r \approx 4$ ; (e)  $t = 378$  s,  $\dot{\gamma} = 3.6$  s $^{-1}$ ,  $\eta_r \approx 5$ ; (g)  $t = 723$  s,  $\dot{\gamma} = 6.0$  s $^{-1}$ ,  $\eta_r \approx 4$ . (b), (d), (f), and (h) are schematics for (a), (c), (e), and (g). Note scale bar. For the micrographs, the flow direction is horizontal and the vorticity direction is vertical.

becomes important. In our case here, we can estimate the copolymer diffusivity by calculating diffusing for a PS molecule having the same molecular weight (200 kg/mol) in a PE matrix. The diffusivity is calculated<sup>39</sup> to be  $\approx 4.1 \times 10^{-13}$  cm $^2$ /s at a shear rate of 2 s $^{-1}$  and 190 °C. Therefore, the Plect number is  $\sim 10^9 \gg 1$ , which indicates that the convection of the copolymer induced by shear flow is much more important. When shear is imposed on the PS drop, the copolymer, P(S-*b*-E), will redistribute its concentration at the interface, with higher concentration at the drop ends and tips.<sup>7</sup> This copolymer concentration gradient results in an interfacial stress gradient along the drop, and therefore, the tips are easier to deform and break up via “tip streaming” and release small droplets into the matrix.

Table 2 summarizes the shear rate ( $\dot{\gamma}$ ), capillary number (Ca), and Deborah number (De) for drop deformation and breakup. For all the systems studied, the capillary number is much greater than 1 because the polymer melt has a high viscosity and the drop size is

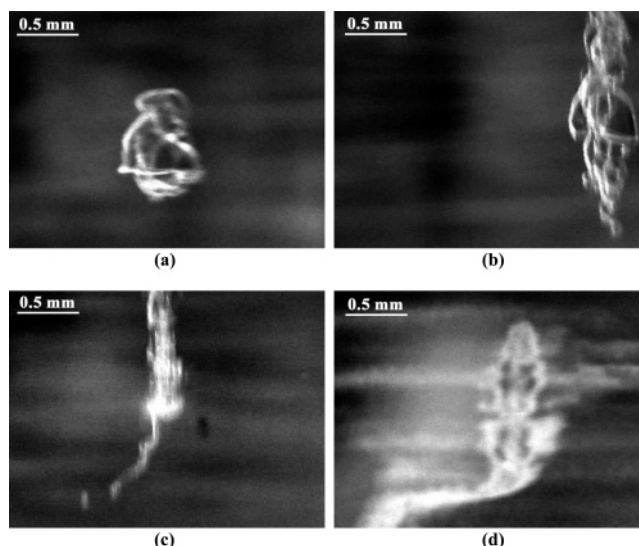


**Figure 7.** Reactive system. Deformation and breakup of a PSOX chunk ( $D_0 \approx 0.60$  mm) inserted inside a PEMA pellet then in a PE2 matrix at 190 °C subject to a stepwise shear rate increase. Time and conditions for each figure: (a)  $t = 0$  s,  $\dot{\gamma} = 0.6$  s $^{-1}$ ,  $\eta_r \approx 6$ ; (b)  $t = 145$  s,  $\dot{\gamma} = 1.9$  s $^{-1}$ ,  $\eta_r \approx 5$ ; (c)  $t = 734$  s,  $\dot{\gamma} = 4.1$  s $^{-1}$ ,  $\eta_r \approx 4$ ; (d)  $t = 1445$  s,  $\dot{\gamma} = 9.7$  s $^{-1}$ ,  $\eta_r \approx 3$ . Note scale bar. For the micrographs, the flow direction is horizontal and the vorticity direction is vertical.

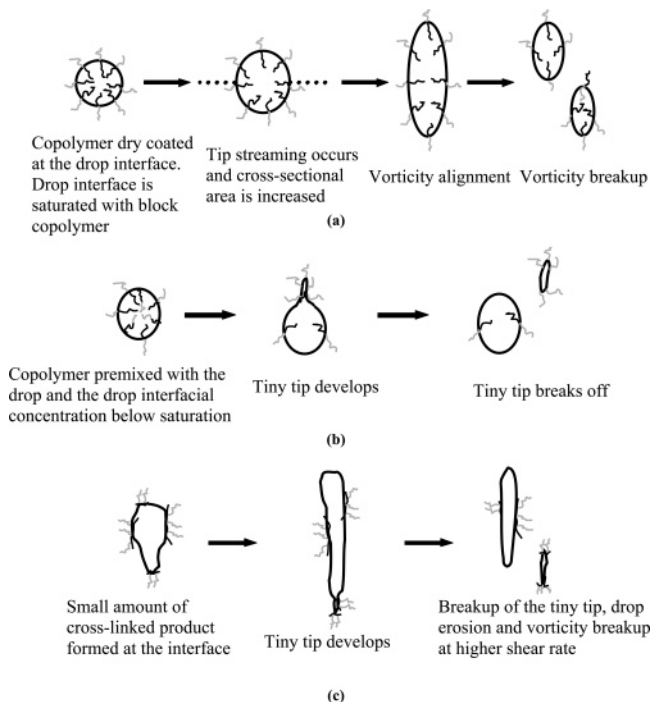


**Figure 8.** Schematics of effect of copolymer and cross-linking reaction on polymer drop breakup. (a) Copolymer is dry coated evenly at the drop surface and the drop surface is saturated with block copolymer. (b) Copolymer is premixed with the drop phase and the drop interfacial concentration is lower than the saturation coverage. (c) Cross-linking reaction takes place gradually and small amount of cross-linked product forms at the interface. For all schematics, the flow direction is horizontal and the vorticity direction is vertical.

in the order of millimeter. Figure 8a,b illustrates the effect of the diblock copolymer on drop deformation and breakup. For PE1/PS, the PS drop exhibits tip streaming, parallel breakup, and vorticity alignment, but no vorticity breakup is seen even when the shear rate is increased to 8 s $^{-1}$ . For PE1/PS with 1% or 5% copolymer,



the drop shows tip streaming and vorticity breakup at shear rate lower than  $8 \text{ s}^{-1}$ . For PE1/PS + 1% P(S-*b*-E), the viscosity ratio of the system is higher than that of the uncompatibilized system, and the drop breaks up in the vorticity direction at a shear rate of around  $7 \text{ s}^{-1}$ . For PE1/PS + 5% P(S-*b*-E), the viscosity ratio is lower than the uncompatibilized system, and we observe that vorticity breakup occurs at a lower shear rate of  $4 \text{ s}^{-1}$ . The lower viscosity ratio may also account for the observed differences between the two copolymer systems, but in both cases, vorticity breakup is observed whereas it is not observed in the uncompatibilized system. In general, for the PS drop (with a diameter of 0.5 mm) without or with copolymer, drop breakup is not so different since the shear rates are comparable, in the range of  $3\text{--}6 \text{ s}^{-1}$ . It suggests that the block copolymer does not facilitate drop breakup as what has been thought in the literature (for example, refs 8–10). In the initial stages of drop breakup, the drop has a bigger size (on the order of 1 mm), where the viscous stress and the normal stresses are more important as compared to the interfacial stress; therefore, the copolymer does not help drop breakup.

However, there are some subtle differences among the systems studied. For example, the drops with premixed copolymer show a slightly higher critical shear rate for breakup than that seen for the drop dry-coated with copolymer. This may be due to the lower interfacial block copolymer concentration and higher concentration gradient for the premixed drop as compared to the dry-coated drop. For a premixed drop with 1% copolymer, a tiny tip is first developed from the mother drop (Table 2) since the interfacial concentration is below the saturation interfacial coverage.<sup>45</sup> For a premixed drop with 5% copolymer, the interfacial coverage is calculated to be  $0.16 \text{ chains/nm}^2$ ,<sup>45,46</sup> which is the maximum interfacial coverage estimated from refs 38 and 42. The mother drop with 5% P(S-*b*-E) is first broken up in the vorticity direction, and then a tiny tip is observed in a daughter droplet. Since interfacial area increases upon breakup, interfacial copolymer concentration may be insufficient to saturate the surface of this smaller droplet. In our experiments, the drop was put into the Couette cell at  $125^\circ\text{C}$ , and then the temperature was increased to  $190^\circ\text{C}$  within 15 min. Once the temperature reached  $190^\circ\text{C}$ , the experiment started. Therefore, the copolymer may not have had sufficient time to distribute itself over the surface at the drop. For drop premixed with copolymer before the experiments, some of the copolymer may still stay inside the drop and the copolymer will most likely be distributed throughout the drop. When the drop is sheared inside the matrix, interfacial concentration gradient arises due to the movement of the copolymer from the drop inside to the drop interface during shearing. After the first drop breakup, some of the daughter droplets may not have enough interfacial coverage of copolymer and concentration gradient exists. As a result, a small tiny cylindrical tip develops due to the accumulation of the copolymers, which increases the local curvature. The interfacial stress is reduced locally, and the interfacial stress gradient increases across the drop, thus increasing the drop Marangoni stress substantially.<sup>6</sup> The drop is resistant<sup>16</sup> to deformation and breakup; therefore, the tiny tip is easier to break up when compared to the drop itself, or in other words, the presence of the tiny tip stabilizes the drop.

For a dry-coated PS drop, all the copolymers are at the drop interface before shearing, and the interfacial concentration is around 80 times that of the saturation coverage before shearing. Though not all the block copolymer will stay at the interface during the experiment, the high initial concentration seems to help keep a significant amount of copolymer at the interface. Because of the high interfacial copolymer concentration, the drop interface is obscured and the drop cross-sectional area is increased (Figure 5b). After the first breakup, the daughter droplets, like their mother drop, may still have sufficient copolymer and less concentration gradient at the interface and therefore break up in the vorticity direction easily.

Therefore, the effect of block copolymer on drop deformation and breakup is slight. It may slightly stabilize the drop by forming a tiny elastic cylindrical tip if there is a copolymer concentration gradient and insufficient interfacial coverage at the interface, as shown in Figures 4 and 8b. It may also help drop area generation and drop breakup if copolymer is saturated and distributes homogeneously across the interface, which is shown for the case of the PS drop coated with P(S-*b*-E) shown in Figures 5 and 8a. The stretching of the drop surface may be attributed to the reduction of interfacial slip and/or the decrease of the interfacial tension.

Table 2 also compares the breakup mechanisms for nonreactive (PE/PSOX) and reactive (PE/PSOX + PEMA) systems. Erosion and vorticity alignment and breakup occur at a lower shear rate for PE/PSOX systems. With PEMA, a tiny cylindrical tip is extended from the mother drop and aligns in the vorticity direction. This tiny tip is similar to that observed for PE/PS premixed with copolymer. The oxazoline in PSOX undergoes a ring-opening reaction with the maleic anhydride<sup>47</sup> in PEMA and leads to cross-linking at the interface. The newly cross-linked PS–PE material may initially act as a copolymer (see Figures 7 and 8c), a rigid protective shell around the drop. A tiny cylindrical tip develops in the vorticity direction as it is seen for the drop premixed with copolymer. This tiny tip stabilizes the drop, and the drop breaks up at a higher shear rate than that for the nonreactive system. The cross-linked interface may also reduce or completely restrict erosion from the drop surface until the shear rate is increased further.

We observed vorticity alignment in all the polymer systems shown in this paper. However, vorticity alignment and breakup cannot be seen in all polymer systems.<sup>45</sup> We have found that uncompatibilized polymer drop can break up at a viscosity ratio higher than 3.5, and the correlation between capillary number and viscosity ratio is not appropriate for polymer drop breakup. This may be due to the shear-thinning and viscoelastic properties of polymers. Normal stresses from both the drop and matrix phases play an important role. Drop vorticity alignment and breakup occur when the drop phase is more elastic than the matrix phase.<sup>45</sup>

## Conclusion

The effect of compatibilizer on polymer drop deformation and breakup was studied in a specially designed transparent Couette mixer. It is found that the presence of premade copolymer does not affect initial polymer drop breakup significantly. PS drops with or without compatibilizer sheared in a PE matrix align and elongate in the vorticity direction. When premade compati-

bilizer (P(S-*b*-E)) is added inside the drop phase (PS), an elastic thin cylindrical tip develops in the vorticity direction and then ruptures from the elongated mother drop. For the case of a PS drop coated with P(S-*b*-E), the drop interface is obscured. For a reactive system, when a PSOX drop is sheared in a PEMA phase, drop breakup occurs at a higher shear rate than the nonreactive system. This may be due to the cross-linking reaction between PSOX and PEMA at the interface, producing a cross-linked copolymer that prevents breakup. All compatibilized drops, except drops coated with copolymer, showed a tiny cylindrical tip and the formation of this tiny tip with high interfacial curvature stabilized the mother drop.

**Acknowledgment.** We thank the Natural Sciences and Engineering Research Council of Canada (NSERC) for financial support of this work. We also thank Mr. Robert Lemieux at NRC-IMI for helping with the experiments. We are grateful to Professors Christopher W. Macosko and Frank S. Bates at University of Minnesota for providing the block copolymer, Dow Chemical for donating PS and PSOX pellets, Petromont for donating the PE pellets, and DuPont for donating the PEMA pellets. B.L. is grateful for the support of a Dissertation Fellowship from University of Alberta.

## References and Notes

- (1) Elmendorp, J. J.; Van der Vegt, A. K. In *Two Phase Polymer Systems*; Utracki, L. A., Ed.; Hanser Publishers: New York, 1991; p 166.
- (2) Utracki, L. A.; Shi, Z. H. *Polym. Eng. Sci.* **1992**, *32*, 1824–1833.
- (3) Utracki, L. A. *Can. J. Chem. Eng.* **2002**, *80*, 1008–1016.
- (4) Levitt, L.; Macosko, C. W. *Macromolecules* **1999**, *32*, 6270–6277.
- (5) van Puyvelde, P.; Velankar, S.; Mewis, J.; Moldenaers, P. *Polym. Eng. Sci.* **2002**, *42*, 1956–1964.
- (6) Velankar, S.; van Puyvelde, P.; Mewis, J.; Moldenaers, P. *J. Rheol.* **2004**, *48*, 725–744.
- (7) Jeon, H. K.; Macosko, C. W. *Polymer* **2003**, *44*, 5381–5386.
- (8) Milliken, W. J.; Stone, H. A.; Leal, L. G. *Phys. Fluids A* **1993**, *5*, 69–79.
- (9) Milliken, W. J.; Leal, L. G. *J. Colloid Sci.* **1994**, *166*, 275–285.
- (10) Tretheway, D. C.; Leal, L. G. *AIChE J.* **1999**, *45*, 929–937.
- (11) Sundararaj, U.; Macosko, C. W. *Macromolecules* **1995**, *28*, 2647–2657.
- (12) Hu, Y. T.; Pine, D. J.; Leal, L. G. *Phys. Fluids* **2000**, *12*, 484–489.
- (13) Velankar, S.; van Puyvelde, P.; Mewis, J.; Moldenaers, P. *J. Rheol.* **2001**, *45*, 1007–1019.
- (14) Lin, B.; Sundararaj, U.; Mighri, F.; Huneault, M. A. *SPE ANTEC Technol. Pap.* **2003**.
- (15) Lin, B.; Sundararaj, U.; Mighri, F.; Huneault, M. A. *Polym. Eng. Sci.* **2003**, *43*, 891–904.
- (16) Lin, B.; Mighri, F.; Huneault, M. A.; Sundararaj, U. *Macromol. Rapid Commun.* **2003**, *24*, 783–788.
- (17) Taylor, G. I. *Proc. R. Soc. London, Ser. A* **1934**, *146*, 501–523.
- (18) Grace, H. P. *Chem. Eng. Commun.* **1982**, *14*, 225–277.
- (19) Potente, H.; Bastian, M.; Bergemann, K.; Senge, M.; Scheel, G.; Winkelmann, Th. *Polym. Eng. Sci.* **2001**, 222–231.
- (20) Scott, C. E.; Macosko, C. W. *Polym. Bull. (Berlin)* **1991**, *26*, 341–348.
- (21) Lindt, J. T.; Ghosh, A. K. *Polym. Eng. Sci.* **1992**, *32*, 1802–1813.
- (22) Sundararaj, U.; Macosko, C. W.; Rolando, R. J.; Chan, H. T. *Polym. Eng. Sci.* **1992**, *32*, 1814–1823.
- (23) Sundararaj, U.; Dori, Y.; Macosko, C. W. *SPE ANTEC Technol. Pap.* **1994**, *52*, 2448–2451.
- (24) Scott, C. E.; Macosko, C. W. *Polymer* **1995**, *36*, 461–470.
- (25) Sundararaj, U.; Dori, Y.; Macosko, C. W. *Polymer* **1995**, *36*, 1957–1968.
- (26) Sundararaj, U.; Macosko, C. W.; Shih, C. K. *Polym. Eng. Sci.* **1996**, *36*, 1769–1781.
- (27) Hobbie, E. K.; Migler, K. B. *Phys. Rev. Lett.* **1999**, *82*, 5393–5396.
- (28) Migler, K. B.; Hobbie, E. K.; Qiao, F. *Polym. Eng. Sci.* **1999**, *39*, 2282–2291.
- (29) Migler, K. B. *J. Rheol.* **2000**, *44*, 277–290.
- (30) Mighri, F.; Huneault, M. A. *J. Rheol.* **2001**, *45*, 783–797.
- (31) Cherdhirankorn, T.; Lerdwijitjarud, W.; Sirivat, A.; Larson, R. G. *Rheol. Acta* **2004**, *43*, 246–256.
- (32) Lerdwijitjarud, W.; Sirivat, A.; Larson, R. G. *J. Rheol.* **2004**, *48*, 843–862.
- (33) Bartok, W.; Mason, S. G. *J. Colloid Sci.* **1959**, *14*, 13–26.
- (34) Rumscheidt, F. D.; Mason, S. G. *J. Colloid Sci.* **1961**, *16*, 238–261.
- (35) de Bruijn, R. A. *Chem. Eng. Sci.* **1993**, *48*, 277–284.
- (36) Milliken, W. J.; Leal, L. G. *J. Non-Newtonian Fluid Mech.* **1991**, *40*, 355–379.
- (37) Milliken, W. J.; Leal, L. G. *J. Non-Newtonian Fluid Mech.* **1992**, *42*, 231–239.
- (38) Lyu, S.; Jones, T. D.; Bates, F. S.; Macosko, C. W. *Macromolecules* **2002**, *35*, 7845–7855.
- (39) van Krevelen, D. W. *Properties of Polymers*, 2nd ed.; Elsevier Scientific Company: Amsterdam, 1976.
- (40) Elemans, P. H. M.; Janssen, J. M. H.; Meijer, H. E. H. *J. Rheol.* **1990**, *34*, 1311–1325.
- (41) Breuer, O.; Sundararaj, U.; Toogood, R. W. *Polym. Eng. Sci.* **2004**, *44*, 868–879.
- (42) Bates, F. S.; Fredrickson, G. H. *Phys. Today* **1999**, *52*, 32–38.
- (43) Jones, T. D.; Bates, F. S.; Macosko, C. W. *Polym. Prepr. Am. Chem. Soc.* **1999**, *40*, 1097–1098.
- (44) Zhao, R.; Macosko, C. W. *J. Rheol.* **2002**, *46*, 145–167.
- (45) Lin, B. Ph.D. Thesis, University of Alberta, 2005.
- (46) Matos, M.; Favis, B. D.; Lomellini, P. *Polymer* **1995**, *36*, 3899–3907.
- (47) Liu, N. C.; Baker, W. E.; Russell, K. E. *J. Appl. Polym. Sci.* **1990**, *41*, 2285–2300.

MA0476240